

# Influences of ageing parameters on the microstructure and mechanical properties of extruded 6063 and 6005 alloys

Do Van Quang<sup>1\*</sup>, Le Thi Van Anh<sup>1</sup>, Vu Thi Huong Ly<sup>1</sup>, Nguyen Quoc Tuan<sup>2</sup>

<sup>1</sup>Department of Metallurgy Technology, National Institute of Mining - Metallurgy Science and Technology,  
4 Pham Van Dong Street, Mai Dich Ward, Cau Giay District, Hanoi, Vietnam

<sup>2</sup>Faculty of Industrial Systems, School of Mechanical and Automotive Engineering, Hanoi University of Industry,  
298 Cau Dien Street, Cau Dien Ward, Bac Tu Liem District, Hanoi, Vietnam

Received 26 February 2024; revised 21 March 2024; accepted 26 April 2024

## **Abstract:**

The influences of ageing time and ageing temperature on the microstructure and mechanical properties were investigated for the extruded 6063 and 6005 alloys. Artificial ageing was performed on the alloy extrusions. The ageing process for 6063 aluminium alloy extrusions was studied at temperatures of 190, 205, and 220°C for durations of 90, 150, and 210 minutes, while extruded 6005 alloys were treated at temperatures of 150, 175, and 200°C for 4, 8, and 12 hours. The results demonstrate that the coarse AlMeSi particles formed during extrusion evolved from granular to rod-like particles (AlFeSi) as the ageing temperature or time increased for both aluminium alloy extrusions, with spherical particles (Al(Mn,Cr,Mg)Si) observed in the 6005 aluminium alloy extrusions. The mechanical properties of the extrusions at room temperature were highly sensitive to the ageing process. The optimal tensile strength, elongation, and hardness for the extruded 6063 and 6005 alloys were achieved at 190°C after 150 minutes and at 175°C after 8 hours, respectively.

**Keywords:** ageing, aluminium alloy, mechanical properties, microstructure.

**Classification numbers:** 2.1, 2.2, 2.3

## **1. Introduction**

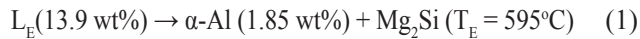
Aluminium alloys are highly desirable for structural applications due to their high strength-to-weight ratio, ease of machining and extrusion, excellent corrosion resistance, thermal and electrical conductivity, and recyclability. It is estimated that 78% of all extracted aluminium remains in use today, and recycling aluminium requires only 5% of the energy used in its original extraction [1]. These properties have driven the increased use of aluminium in the automotive industry. The two most commonly used aluminium alloys, 6005 and 6063, are alloyed with magnesium and silicon. As heat-treatable alloys, they can undergo post-extrusion heat treatments to increase strength via precipitation hardening. Alloy 6005 is a benchmark structural alloy known for its high strength, toughness, and ease of anodisation and machining. While 6063 alloy is not as tough or strong as 6005, it offers superior surface appearance and formability [2]. Although 7xxx series alloys are another option for structural aluminium, their poor extrudability makes them cost-prohibitive for many applications [1].

Due to their excellent extrusion performance, good welding characteristics, high corrosion resistance, and moderate strength, the 6063 and 6005 aluminium alloys

are widely used across industries such as machinery manufacturing, aerospace, aviation, and transportation, including in high-speed trains, subways, and urban railways [2, 3]. These alloys can be extruded to produce complex sectional shapes with thin walls and quenched via air or water mist cooling, making them one of the most commonly used materials for vehicle body construction [4-6]. However, 6005 alloy exhibits high quench sensitivity, requiring ageing treatments post-extrusion to achieve stable microstructures and mechanical properties [7-9]. To quickly achieve high-strength extrusions, artificial ageing is commonly employed in industrial production.

The appropriate ageing process and microstructure are key to achieving superior comprehensive mechanical properties in extruded 6063 and 6005 alloys. These alloys belong to the excess Si-strengthened Al-Mg-Si series. In the ternary Al-Mg-Si system, Mg<sub>2</sub>Si particles form via a ternary peritectic reaction. However, in the pseudo-binary Al-Mg<sub>2</sub>Si system, obtained from a vertical section of the Al-Mg-Si ternary system at a fixed Mg:Si atomic ratio of 2:1 (equivalent to 1.73:1 when the same ratio is expressed as a quotient of weights [10], Mg<sub>2</sub>Si particles form as equilibrium reaction products from a eutectic reaction [11]:

\*Corresponding author: Email: dovanquang@vimluki.vn



where the concentrations are expressed in weight percent of  $\text{Mg}_2\text{Si}$ . Given that the Mg limits the solubility of  $\text{Mg}_2\text{Si}$  in  $\alpha\text{-Al}$ , while the Si has no effect on it, a weight ratio of  $\text{Mg}:\text{Si} \leq 1.73$  is desirable when designing industrial alloys in order to ensure the maximum amount of this compound in solution [12]. Assuming that all the Mg is present in the  $\text{Mg}_2\text{Si}$  form, the amount of Si needed to form  $\text{Mg}_2\text{Si}$  precipitates for the compositional range of Mg in 6xxx alloys is given by [10]:

$$[\text{Si}]_{\text{Mg}_2\text{Si}} = [\text{Mg}]_{\text{total}} \times \frac{A_{\text{Si}}}{2x A_{\text{Mg}}} \quad (\text{wt}\%) \quad (2)$$

where  $[\text{Si}]_{\text{Mg}_2\text{Si}}$  is the amount of Si expressed in wt% present in the  $\text{Mg}_2\text{Si}$  compound;  $[\text{Mg}]_{\text{total}}$  corresponds to Mg interval values for 6xxx alloys; and  $A_{\text{Si}}$  and  $A_{\text{Mg}}$  are the atomic weights of Si and Mg, respectively.

The  $\text{Mg}_2\text{Si}$  concentration,  $[\text{Mg}_2\text{Si}]$ , can be calculated according to:

$$[\text{Mg}_2\text{Si}] = [\text{Si}]_{\text{Mg}_2\text{Si}} + [\text{Mg}]_{\text{total}} \quad (\text{wt}\%) \quad (3)$$

As far as alloying is concerned, it appears that the amount of the so-called excess Si (Siex) is important as it affects the precipitation kinetics in Al-Mg-Si alloys. Siex leads to finer and denser precipitates by enhancing the nucleation kinetics of GP zones. It has been reported that the excess Si in the alloy enhances the nucleation of the hexagonal  $\beta\text{-Mg}_2\text{Si}$  on Si atom grids, which are composed of hexagonal sub cells with lattice parameters  $a=b=4.05 \text{ \AA}$  and  $c=4.05 \text{ \AA}$  [13]. For a given Mg and Fe content, the amount of Siex depends on which intermetallic ( $\alpha\text{-AlFeSi}$  or  $\beta\text{-AlFeSi}$ ) is present [10]:

$$[\text{Si}]_{\text{xs}} = [\text{Si}]_{\text{alloy}} - [\text{Si}]_{\alpha\text{-AlFeMnSi}} - [\text{Si}]_{\text{Mg}_2\text{Si}} \quad (4)$$

$$[\text{Si}]_{\alpha\text{-AlFeMnSi}} = [\text{Fe}+\text{Mn}]_{\text{alloy}} \times \frac{A_{\text{Si}}}{3x(A_{\text{Mg}}+A_{\text{Mn}})} = 0.0664 [\text{Fe}+\text{Mn}]_{\text{alloy}} \quad (5)$$

As a heat-treatable aluminium alloy, precipitation strengthening is the primary strengthening mechanism in these alloys [14]. The precipitation phases vary with different ageing temperatures and times. At low temperatures and short times, solute atom clusters (GP zones) are difficult to form, resulting in low post-ageing strength (under-ageing). Conversely, at high temperatures and extended times, the critical nucleus size increases, leading to low strength after ageing (over-ageing).

Prior to the ageing process, the alloy undergoes solution treatment at elevated temperatures to dissolve the second-phase particles and maintain the elements in a single-phase ( $\alpha$ ) region. This is followed by quenching, which prevents the precipitation of the second phase, trapping the alloying elements in the  $\alpha$  phase and producing a supersaturated solid solution (SSSS). During the ageing process, these alloying elements diffuse from the SSSS to form strengthening precipitates [15]. This nucleation is driven by the reduction

in Gibbs free energy as the thermodynamically unstable SSSS transforms into a more stable two-phase state. For 6xxx aluminium alloys, the artificial ageing temperature/time range is typically between 165 and 205°C for 2 to 16 hours, which is considered optimal for mechanical properties across a variety of applications [16].

While several types of precipitates can form during ageing, three main categories are typically considered, depending on the nature of the interface between the precipitates and the matrix. Coherent precipitates form when the atomic lattice of the precipitate aligns perfectly with the matrix lattice across the interface. Semi-coherent precipitates occur when the majority of the lattices match across the interface, though the mismatch is sufficient to accommodate dislocations. Lastly, incoherent precipitates do not align with the matrix at all [17].

Smaller precipitates with narrow inter-particle spacing generally provide optimal strengthening by creating strain fields that interact with dislocations, thereby hindering their motion. As precipitate size increases, the energy required for dislocation cutting also increases, leading to dislocation bowing around the precipitates. Additionally, as the inter-particle spacing grows, dislocations can more easily bow around the precipitates, forming a dislocation loop that obstructs other dislocations and favours the dislocation-cutting mechanism. To achieve optimal alloy strength, the aim is to determine the ageing time and temperature at which the cutting and bowing mechanisms result in equivalent strength. At this point, the alloy reaches its maximum strength [18].

Previous studies primarily focused on optimising composition, the extrusion process, quenching sensitivity, and welding in 6063 and 6005 alloys [6, 7, 19-23]. However, limited research has been conducted on the ageing process [22-29], particularly regarding short-term, single-stage ageing, which is advantageous in reducing production cycles and costs. To enhance the mechanical properties of extrusions while minimising energy consumption, the short-term ageing process can be optimised to achieve the best age-hardening effect in extruded 6063 and 6005 alloys. In this study, the influences of ageing temperature and time on the microstructure and mechanical properties of extruded 6063 and 6005 alloys were investigated under various short-term, single-stage ageing conditions.

## 2. Materials and methods

The 6063 and 6005 aluminium alloys in the form of extruded profiles with a thickness of 18 mm and a width of 80 mm were supplied by VietY Aluminium Company Limited. The chemical compositions of the experimental alloys, compared with the standard 6063 and 6005 alloys, are presented in Table 1.

**Table 1. Chemical composition of 6063 and 6005 aluminium alloys.**

Alloy	Si	Fe	Cu	Mn	Mg	Cr	Zn	Ti	Al
6063	0.486	0.236	0.028	0.023	0.547	0.012	0.022	0.023	Remain
6005	0.853	0.235	0.036	0.024	0.675	0.014	0.027	0.023	Remain

The extruded profiles were produced following the online solid solution and quenching process. The extrusion coefficient ranged between 18 and 20, with an extrusion speed of 5 mm/s and an extrusion temperature of 510-540°C. Online air cooling quenching was applied for the 6063 alloys, while water cooling quenching was employed for the 6005 alloys during the extrusion process.

The ageing treatments for the 6063 and 6005 aluminium alloys are illustrated in Figs. 1 and 2. The 6063 alloys were aged at 190, 205, and 220°C for 90, 150, and 210 minutes, respectively. Meanwhile, the 6005 alloys were aged at 150, 175, and 200°C for 4, 8, and 12 hours, respectively.

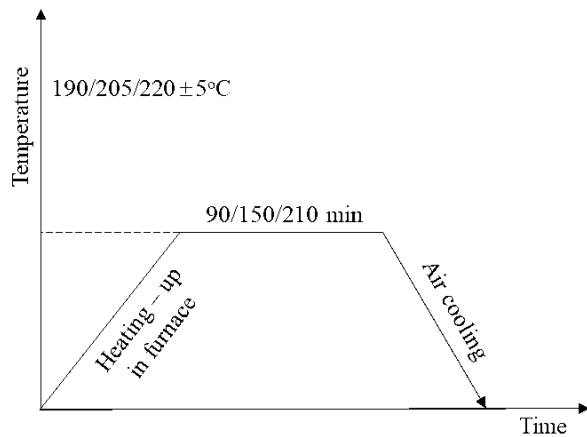


**Fig. 1. Aging conditions of 6063 aluminium alloy.**

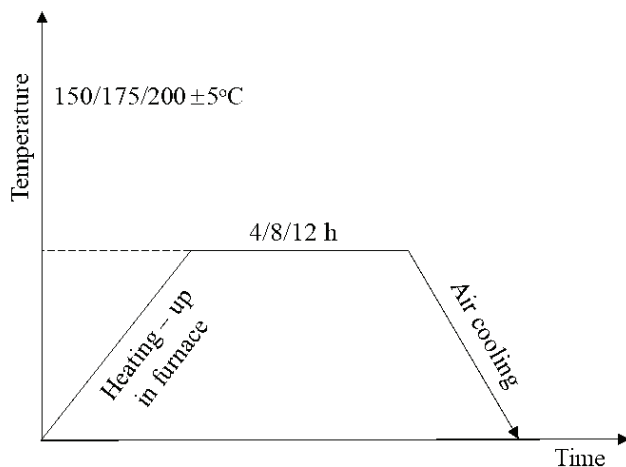


**Fig. 2. Aging conditions of 6005 aluminium alloy.**

The extruded profiles were sectioned transversely for microstructure observation and longitudinally for mechanical properties testing. The final tensile strength values were averaged from three tests, conducted at a strain rate of 1/20 mm/s using a YMM-5 testing apparatus. The tensile specimens were prepared according to ASTM E557M standards [2].

Hardness was measured at room temperature using a Brinell hardness testing machine with a 62.5 N load. The final hardness value was the average of five tests performed at various points evenly distributed from the outermost point to the centre of the specimen.

The microstructure of the samples was examined using both optical and scanning electron microscopes (SEM) with an energy-dispersive X-ray spectroscopy (EDS) detector. The samples were initially polished with 1200-grit paper and then polished using an alumina-containing colloidal suspension. Following polishing, the samples were inspected under both pre- and post-etching conditions. The etching process was conducted using Keller's solution (85 ml H<sub>2</sub>O, 10 ml HNO<sub>3</sub>, and 5 ml HF) for 30 seconds. The samples were then rinsed with deionised water and alcohol, dried, and examined under optical and scanning electron microscopes.

### 3. Results and discussion

Figure 3 presents optical microscopy images of the 6063 and 6005 aluminium alloys. Specifically, the former was aged at 205°C for 150 minutes, while the latter was aged at 175°C for 8 hours. The particle sizes in both alloys were inhomogeneous, with the largest particles measuring approximately 100 µm. Overall, altering the ageing temperature and time for either aluminium alloy did not significantly affect grain size.

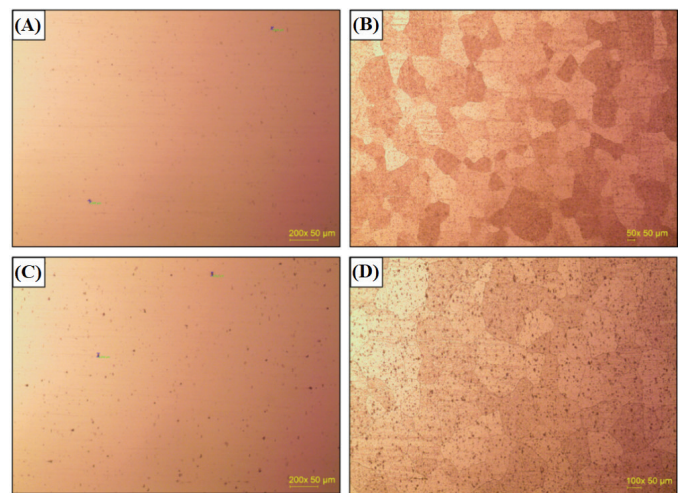


**Fig. 3. (A, B) Optical microscope images of 6063 aluminium alloy aged at 205°C and held for 150 minutes, before and after etching, respectively; (C, D) 6005 aluminium alloy aged at 175°C and held for 8 hours, before and after etching, respectively.**

During the high-temperature ageing process, precipitates developed at an accelerated rate. Through SEM and EDS analyses (Figs. 4 and 5) of the 6063 alloy, it was observed that precipitates formed spherical structures containing Cr and Fe at lower ageing temperatures, as shown in the EDS analysis in Fig. 4. These precipitates were identified as AlFeSi and AlCrSi particles, with a size of approximately 1  $\mu\text{m}$ . However, increasing the ageing temperature altered the precipitate form, with AlFeSi particles observed as rod-like structures, and some spherical precipitates containing Ni, Cr, and Mn, as shown in Fig. 5.

SEM images and EDS analysis of the 6005 aluminium alloy, which was aged at 175 and 200°C, are presented in Figs. 6 and 7. The results show that, when aged at lower temperatures, precipitates formed in relatively small sizes, with  $\text{Mg}_2\text{Si}$  particles as spherical structures or AlFeSi as bar-like forms (Fig. 6). As the ageing temperature increased, the precipitate size increased slightly, while their shape remained unchanged (Fig. 7). The spherical precipitates contained Mn, Mg, or Cr, and their sizes ranged from 0.5 to 1  $\mu\text{m}$ . AlFeSi particles were also observed as rod-like structures, similar to those in the 6063 aluminium alloy.

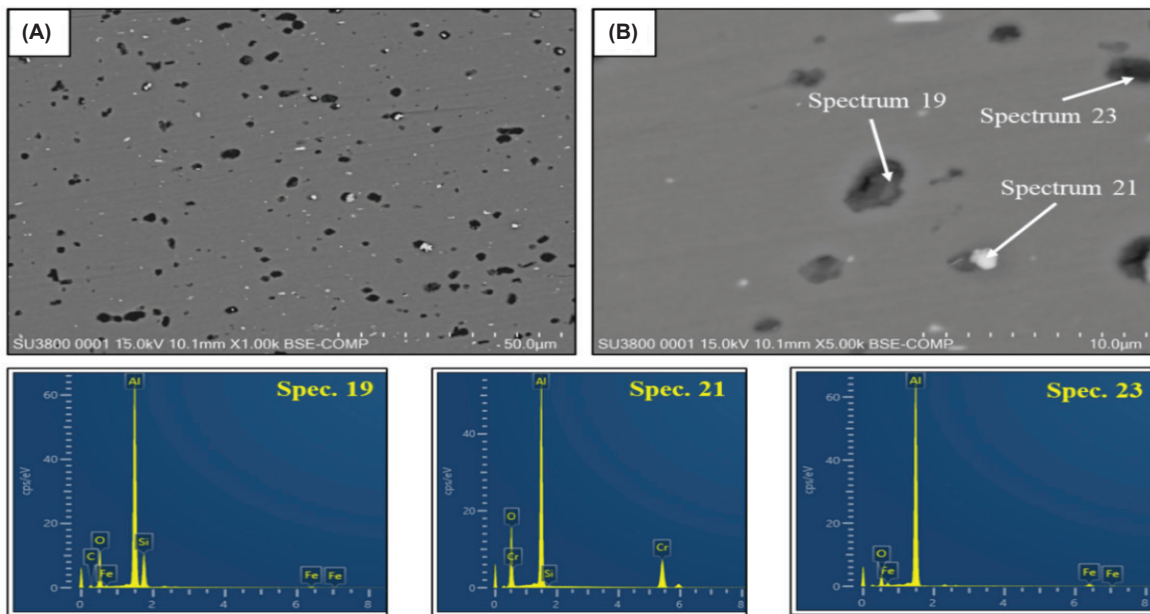


Fig. 4. SEM image of 6063 aluminium alloy aged at 190°C and held for 150 minutes, before etching (A) low magnification, (B) high magnification and EDS analysis for each spectrum.

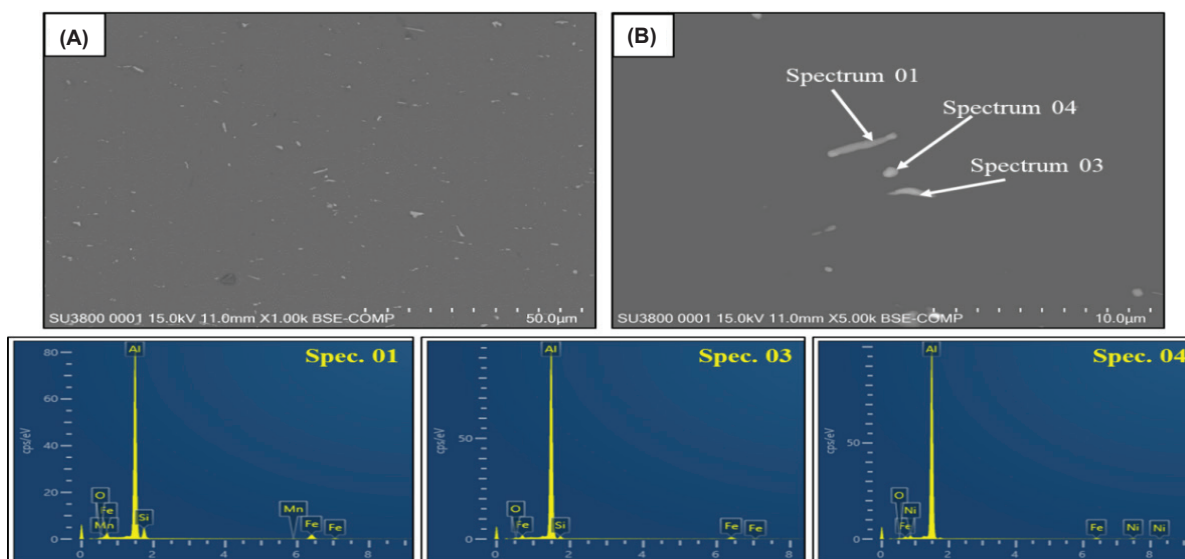
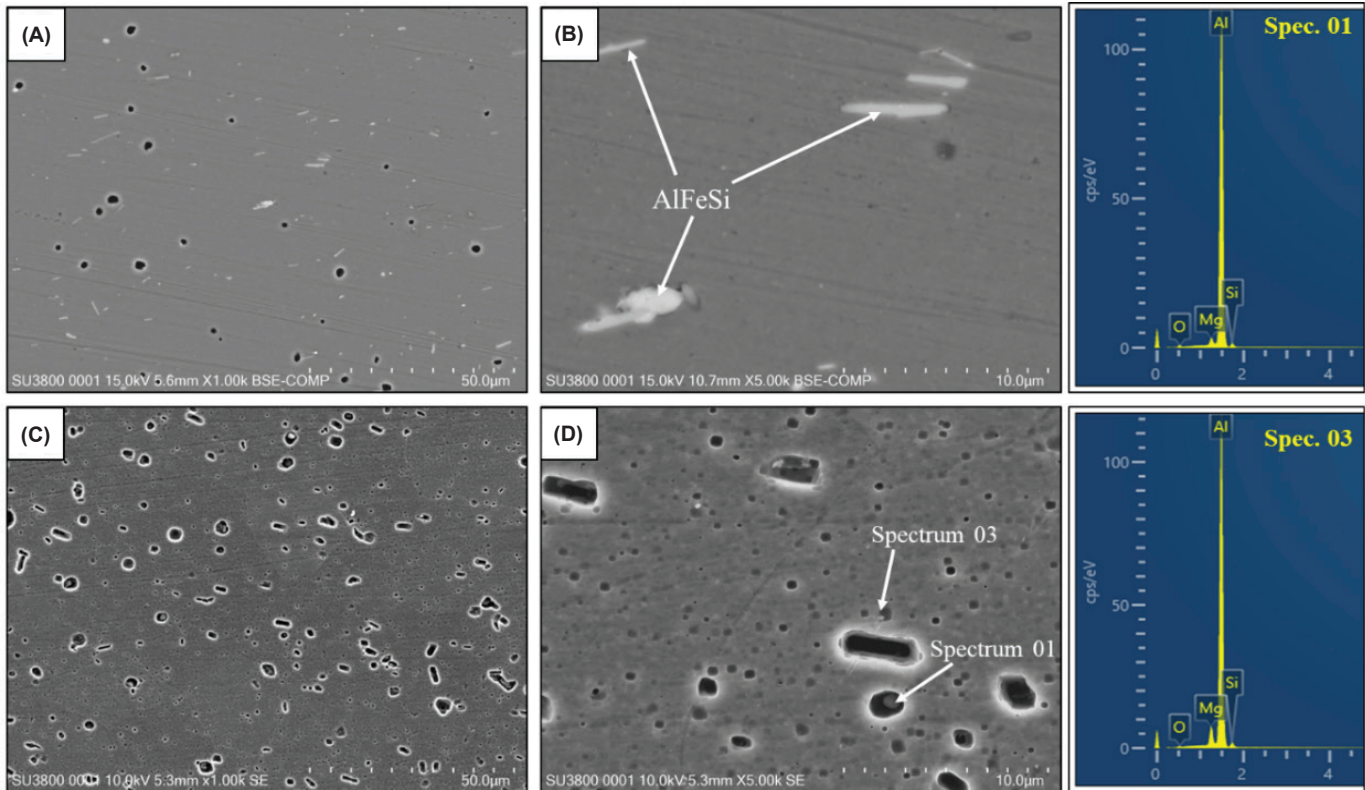


Fig. 5. SEM image of 6063 aluminium alloy aged at 205°C and held for 150 minutes, before etching (A) low magnification, (B) high magnification and EDS analysis for each spectrum.



**Fig. 6. SEM images and EDS analysis of 6005 aluminium alloy aged at 175°C and held for 8 hours, (A, B) before etching and (C, D) after etching.**

The precipitates described above had a direct influence on the mechanical properties of the 6063 and 6005 aluminium alloys. Their formation during the ageing process enhanced the strength of the alloys due to the interaction between dislocation motion and the precipitates.

Peak ageing is one of the ageing treatment methods extensively used in current industrial applications. It produces the highest density of precipitates in the matrix, thereby maximising the strength of the alloys. The kinetics of ageing is controlled by the diffusion of solute atoms, which is strongly dependent on the temperature and duration of the ageing process. Precipitates clearly play a crucial role in determining the mechanical properties of the 6005 and 6063 aluminium alloys. The strengthening effect is closely related to the type, interface, morphology, density, and size of the precipitates. Coarse particles larger than 3 µm are typically formed during the extrusion process, comprising Fe-containing inclusions such as AlFeSi and Al(Fe,Cr)Si [8, 30]. As

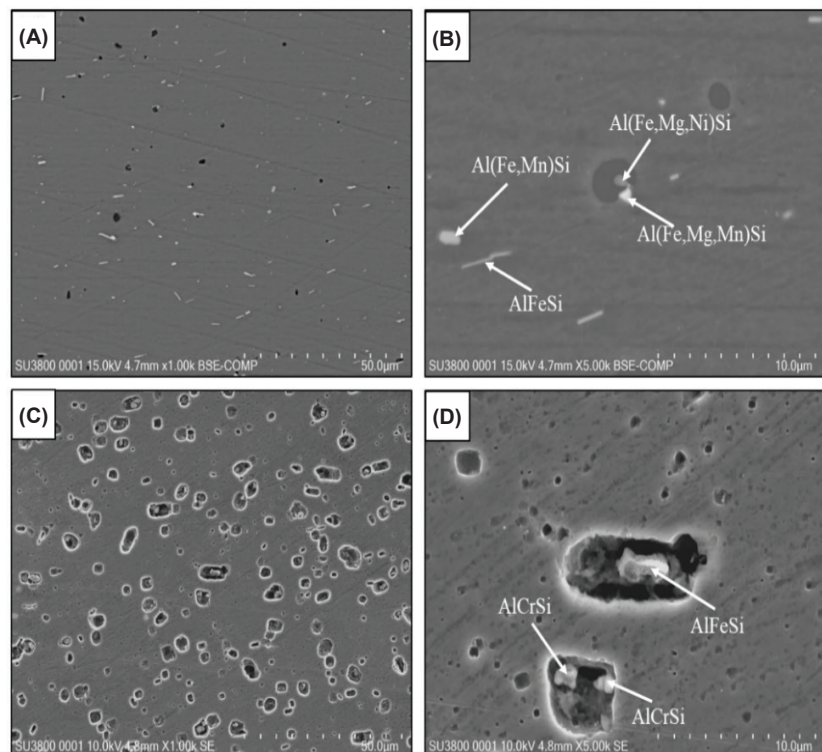


**Fig. 7. SEM images of 6005 aluminium alloy aged at 200°C and held for 8 hours (A, B) before etching and (C, D) after etching.**

shown in Figs. 2 to 7, increasing the time and temperature during ageing caused slight changes in the size and morphology of the coarse particles due to thermal diffusion at the phase interface. Submicron precipitates are expected to form during the ageing process [31]. Under short-term, single-stage ageing, the quantity and size of the submicron precipitates depended on the temperature and duration of the process.

Figures 8 and 9 illustrate the influence of temperature and holding time during the ageing process on the hardness of the 6063 and 6005 aluminium alloys. For the 6063 alloy (Fig. 8), hardness gradually increased with extended ageing time. After 2.5 hours of ageing, the hardness remained unchanged regardless of the temperature. In contrast, the hardness of the 6005 alloy decreased as the ageing time increased, with a more pronounced decline at lower temperatures compared to higher temperatures (Fig. 9). The hardness values obtained for the 6005 and 6063 alloys through this ageing process aligned with commercial standards.

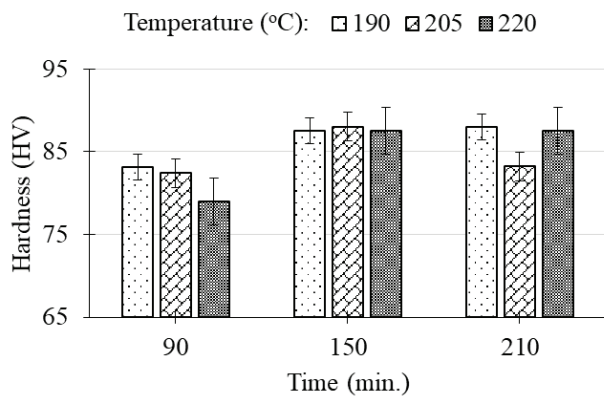


Fig. 8. The dependence of 6063 aluminium alloy hardness on temperature and hold time of ageing.

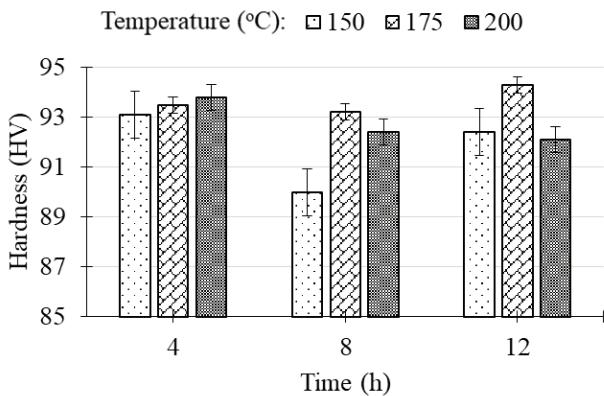


Fig. 9. The dependence of 6005 aluminium alloy hardness on temperature and hold time of ageing.

The rapid age-hardening response observed after 1.5 hours of ageing at 190°C for the 6063 alloy (Fig. 8) and 4 hours at 175°C for the 6005 alloy (Fig. 9) reflects the initial fast formation of GP zones and Mg-Si co-clusters, which were trapped during water-mist cooling. This precedes the formation of needle-shaped  $\beta''$ -strengthening precipitates, which are partially or fully coherent with the matrix, significantly improving the mechanical properties as seen in the ageing curves. The participation of Mg and Si solute atoms in these precipitation events reduces the availability of solute atoms for further precipitation, leading to a reduction in strengthening over time. Additionally, the slow increase in hardness between 2.5 to 3.5 hours for the 6063 alloy and 8 to 12 hours for the 6005 alloy could be attributed to the formation of incoherent and larger, less effective rod-shaped  $\beta'$  and  $\beta$  precipitates. The lower hardness values observed after ageing, as shown in Figs. 8 and 9, could be attributed to supersaturation or low vacancy concentrations during the extrusion process, which may have impeded the formation of significant strengthening phases during ageing [32-35].

Figures 10 and 11 show the tensile strength of the 6063 and 6005 aluminium alloys as a function of ageing parameters. As ageing time increased, tensile strengths of both alloys increased at the lowest temperature (190°C) but decreased at higher temperatures. Notably, the tensile strength of the 6063 alloy aged at 205°C reached a peak of 248.02 MPa at 2.5 hours before declining. In the case of the 6005 alloy, despite initial differences, tensile strengths converged at values above 250 MPa after 12 hours of ageing, irrespective of temperature (Fig. 11). The highest tensile strength for the 6005 alloy, 268.53 MPa, was achieved by ageing at 175°C for 4 hours.

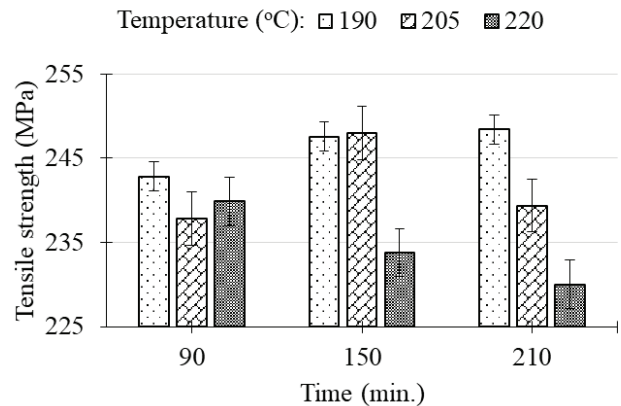
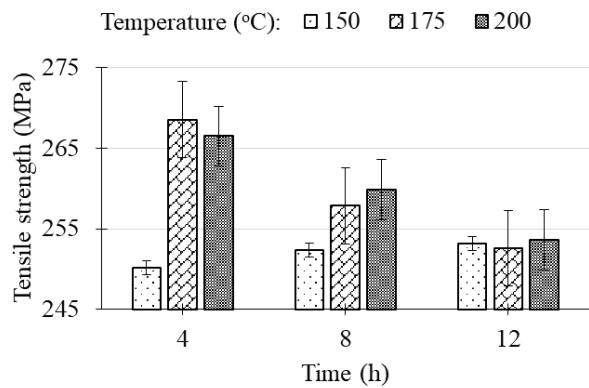
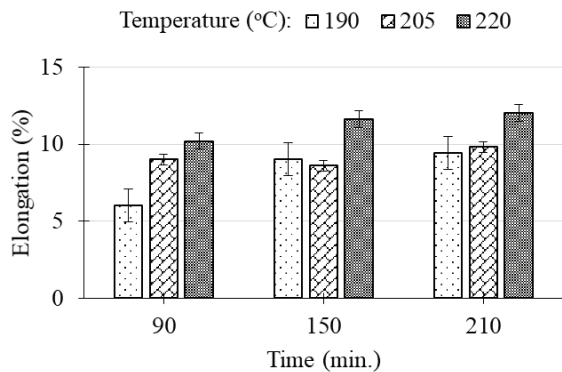


Fig. 10. The tensile strength of the 6063 aluminium alloy as a function of ageing temperature and holding time.



**Fig. 11.** Tensile strength of the 6005 aluminium alloy as a function of ageing temperature and holding time.



**Fig. 12.** Elongation of the 6063 aluminium alloy as a function of ageing time and temperature.

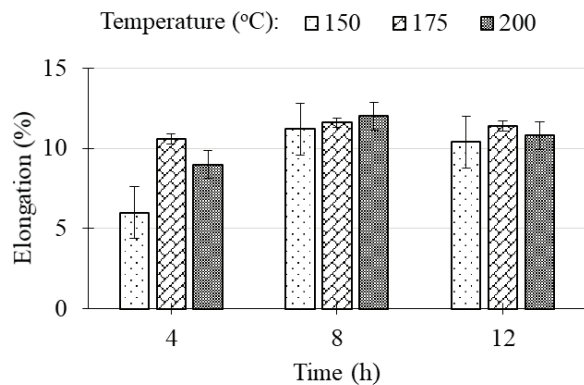


**Fig. 13.** Elongation of the 6005 aluminium alloy as a function of ageing time and temperature.

Figures 12 and 13 show the influence of time and temperature on the elongation of the 6063 and 6005 alloys. Both alloys exhibited increased elongation with longer ageing times and higher temperatures. The 6063 alloy achieved its maximum elongation of 12% after 3.5 hours of ageing at 220°C. Similarly, the 6005 alloy attained the highest elongation (12%) after 8 hours at any of the tested ageing temperatures, with a slight reduction after 12 hours of ageing.

The results above indicate that the mechanical properties of the aluminium alloys are closely linked to their microstructure. Increasing the temperature and ageing time led to grain growth, promoted the formation of precipitates, and had a significant effect on the material’s mechanical properties. The small size of the ageing precipitates allowed dislocations to easily cut through them, which facilitated dislocation movement along the channel and reduced the ductility of the alloy [7]. The evolution of coarse Al(Fe,Cr) Si precipitates from granular to rod-like particles is likely to cause stress concentrations, particularly when AlFeSi particles form at grain boundaries during high-temperature ageing. These particles can further reduce the strength of the extruded alloys [36].

#### 4. Conclusions

This study investigated the effects of temperature and ageing time on the microstructure and mechanical properties of extruded 6063 and 6005 alloys. Precipitates formed rapidly during the high-temperature ageing process in both alloys. These precipitates included rod-like AlFeSi particles, while spherical precipitates consisted of fine Mg<sub>2</sub>Si particles and Cr-, Ni-, and Mn-containing particles, with sizes ranging from 0.5 to 1 μm. The presence of these precipitates in the matrix significantly enhanced the mechanical properties of the extruded 6063 and 6005 alloys.

The mechanical properties of the extruded 6063 alloy at room temperature were highly sensitive to the ageing temperature and duration. Optimal and stable mechanical properties were achieved with an ageing process of 190°C for 2.5 hours for the 6063 alloy, and 175°C for 8 hours for the 6005 alloy. The hardness, tensile strength, and elongation values of the 6063 alloy aged at 190°C for 2.5 hours were 87.5 HV, 247.6 MPa, and 9%, respectively. Meanwhile, the 6005 alloy aged at 175°C for 8 hours achieved a hardness of 93.2 HV, a tensile strength of 257.8 MPa, and an elongation of 11.6%.

#### CRediT author statement

Do Van Quang: Conceptualisation, Methodology, Validation, Formal analysis, Data curation, Visualisation, Supervision, Writing - Reviewing, and Editing; Le Thi Van Anh: Formal analysis; Vu Thi Huong Ly: Formal analysis and Editing; Nguyen Quoc Tuan: Formal analysis.

#### ACKNOWLEDGEMENTS

This work was funded by the Department of Industry, Ministry of Industry and Trade under the grant number 34/2023/HD-CN/CNHT.

#### COMPETING INTERESTS

The authors declare that there is no conflict of interest regarding the publication of this article.

## REFERENCES

- [1] K.H. Matucha (1996), *Structure and Properties of Nonferrous Alloys*, Wiley-VCH, 837pp.
- [2] Y. Wenchao, W. Mingpu, S. Xiaofei, et al. (2010), "Study of the aging precipitation and hardening behavior of 6005A alloy sheet for rail traffic vehicle", *Acta Metallurgica Sinica*, **46**(12), pp.1481-1487, DOI: 10.3724/SP.J.1037.2010.00223.
- [3] Y.L. Li (2000), "Properties and processing characteristic of 6005A alloy", *Light Alloy Fabrication Technology*, **28**(6), pp.41-43.
- [4] L. Jingan (2004), "The extrusion of large sized special 6005A aluminum profile", *Light Alloy Fabrication Technology*, **32**(4), pp.36-41.
- [5] Y. Wanming, S. Jian (2006), "On extrusion and heat treatment technique of 6005A alloy for vehicles", *Journal of Chongqing University of Science and Technology: Natural Science Edition*, **8**(1), pp.33-39.
- [6] S. Jian, L. Yanli, Z. Mingfeng (2003), "Effects of press quenching variables on microstructures and mechanical properties of 6005A alloy extrusion sections", *The Chinese Journal of Nonferrous Metals*, **13**(6), pp.1461-1466.
- [7] C.W. Xiao, M.P. Wang, Z.A. Wang, et al. (2003), "Quench sensitivity of 6005A aluminum alloy", *The Chinese Journal of Nonferrous Metals*, **13**(3), pp.635-639.
- [8] H.L. Zi (2001), *Microstructures and Mechanical Properties of AlmgSi Alloys*, Shenyang: Northeastern University.
- [9] Y.W. Chao (2001), *Aged-Hardening Behavior and Microstructural Characterization of Precipitates in AlmgSi: 6005A Alloy*, Central South University.
- [10] J.A. Lozano, B.S. Peña, G.F.V. Voort (2014), "Effect of processing steps on the mechanical properties and surface appearance of 6063 aluminium extruded products", *Materials*, **7**(6), pp.4224-4242, DOI: 10.3390/ma7064224.
- [11] J.R. Davis (1993a), *Aluminum and Aluminum Alloys (ASM Specialty Handbook)*, ASM International, 784pp.
- [12] C. Meng (2010), *Effect of Preheating Condition on Strength of AA6060 Aluminium Alloy for Extrusion*, Master's Thesis, School of Engineering, Auckland University of Technology, 136pp.
- [13] C.D. Marioara, S.J. Andersen, T.N. Stene, et al. (2007), "The effect of Cu on precipitation in Al-Mg-Si alloys", *Philosophical Magazine*, **87**(23), pp.3385-3413, DOI: 10.1080/14786430701287377.
- [14] J.R. Davis (1993b), *ASM Specialty Handbook: Aluminum and Aluminum Alloys*, ASM International, DOI: 10.1361/autb2001p351.
- [15] Y.S. Sato, H. Kokawa, M. Enomoto, et al. (1999), "Microstructural evolution of 6063 aluminium during friction-stir welding", *Metallurgical and Materials Transactions A*, **30**, pp.2429-2437, DOI: 10.1007/s11661-999-0251-1.
- [16] P. Mukhopadhyay (2012), "Alloy designation, processing, and use of AA6XXX series aluminium alloys", *ISRN Metallurgy*, DOI: 10.5402/2012/165082.
- [17] X.Y. Liu, Q.L. Pan, L.Y. Zheng, et al. (2013), "Effect of aging temper on the thermal stability of Al-Cu-Mg-Ag heat-resistant alloy", *Materials & Design*, **46**, pp.360-365, DOI: 10.1016/j.matdes.2012.10.039.
- [18] A.J. Ardell (1985), "Precipitation hardening", *Metallurgical Transactions A*, **16**, pp.2131-2165, DOI: 10.1007/BF02670416.
- [19] W. Ming, W.H. Dong (2011), "Study on microstructure and mechanical properties of welded joint of 6005A alloy by double wire MIG welding", *Hot Working Technology*, **40**(9), pp.144-145.
- [20] C.J. Hui, S.G. Jie (2008), "Research on aging process of AlMgSi alloys", *Shanghai Metals*, **30**(4), pp.16-18.
- [21] D.X. San, L.J. An (2004), "Research and development of large 6005A alloy profiles for subway vehicle", *Aluminum Fabrication*, **19**(4), pp.19-26.
- [22] A. Simar, Y. Brechet, B.D. Meester, et al. (2007), "Sequential modeling of local precipitation, strength and strain hardening in friction stir welds of an aluminum alloy 6005A-T6", *Acta Materialia Sinica*, **55**(18), pp.6133-6143, DOI: 10.1016/j.actamat.2007.07.012.
- [23] A. Simar, Y. Brechet, B.D. Meester, et al. (2008), "Microstructure, local and global mechanical properties of friction stir welds in aluminium alloy 6005A-T6", *Materials Science and Engineering A*, **486**(1-2), pp.85-95, DOI: 10.1016/j.msea.2007.08.041.
- [24] S. Zajac, B. Hutchinson, A. Johanson, et al. (1993), "Microstructure control and extrudability of Al-Mg-Si alloys, micro alloyed with manganese", *J. Phys. IV France*, **3**, DOI: 10.1051/jp4:1993740.
- [25] I. Musulin, O.C. Celliers (1990), "Role of manganese in 6063 alloy and effect of quench sensitivity in 6063", *Proceedings of The TMS Annual Meeting on Light Metal*, **119**, pp.951-954.
- [26] O.E. Okorafor (1991), "Effect of heat treatment on the corrosion resistance of 6063 aluminium alloy", *Corrosion Prevention and Control*, **38**(6), pp.141-144.
- [27] D.M. Jiang, B.D. Hong, T.C. Lei, et al. (1990), "Fatigue fracture behavior of an under-aged Al-Si-Mg alloy", *Scripta Metall.*, **24**(4), pp.651-654, DOI: 10.1016/0956-716X(90)90217-5.
- [28] P.S. Veers, J.A.V.D. Avyle (1992), "Fatigue crack growth from narrow-band Gaussian spectrum loading in 6063 aluminium alloy", *Advances in Fatigue Lifetime Predictive Techniques*, DOI: 10.1520/STP24160S.
- [29] R. Kumar, S.B.L. Garg (1989), "Effect of yield stress and stress ratio on fatigue crack closure in 6063-T6 aluminium alloy", *Int. J. Pressure Vessels Piping*, **38**(4), pp.293-307, DOI: 10.1016/0308-0161(89)90079-3.
- [30] N.C.W. Kuijpers, J. Tirel, D.N. Hanlon, et al. (2003), "Characterization of the  $\alpha$ -Al(FeMn)Si nuclei on  $\beta$ -AlFeSi intermetallics by laser scanning confocal microscopy", *Journal of Materials Science Letters*, **22**, pp.1385-1387, DOI: 10.1023/A:1025734624469.
- [31] I.J. Polmear (2006), "Light alloys: From traditional alloys to nanocrystals", *Elsevier*, 421pp, DOI: 10.1017/S000192400008670X.
- [32] F. Bakare (2019), *Effect of Extrusion Processing on The Microstructure and Mechanical Properties of AA6082 Aluminium Alloys*, Master Thesis, Macquarie University, DOI: 10.25949/20428254.v1.
- [33] G.I.P.D. Silva, R.A.D. Perera, P.V.S.K. Ranasinghe (2013), "Study of the effects of two step age hardening process on mechanical properties of aluminum 6063-T5 alloy", *National Engineering Conference 2013, 19<sup>th</sup> Eru Symposium, Faculty of Engineering, University of Moratuwa, Sri Lanka*, pp.110-113.
- [34] G.M. Nowotnik (2010), "Influence of chemical composition variation and heat treatment on microstructure and mechanical properties of 6xxx alloys", *Archives of Materials Science and Engineering*, **46**(2), pp.98-107.
- [35] T. Wu, X.F. Ding, J. Sun, et al. (2013), "Effects of the aging time and temperature on the microstructures and mechanical properties of 6082 aluminum alloy extrusions", *Advanced Materials Research*, **652-654**, pp.1035-1042, DOI: 10.4028/www.scientific.net/AMR.652-654.1035.
- [36] X. Ding, J. Sun, J. Ying, et al. (2012), "Influences of aging temperature and time on microstructure and mechanical properties of 6005A aluminum alloy extrusions", *Trans. Nonferrous Met. Soc. China*, **22**, pp.s14-s20, DOI: 10.1016/S1003-6326(12)61677-X.